Velocity as an Attribute:
Continuous Velocity Estimation from 3D preSDM CRP Gathers.

Ian F.Jones* & Huibert Baud

First presented at the 1998 EAGE/SEG summer research workshop:
'Depth Imaging of Reservoir Attributes'.

Published in
'First Break'
v19:1, pp19-23,
January 2001

* Corresponding author
Ian F. Jones
GX Technology
Lawrence House
45 High Street, Egham
Surrey TW20 9DP
Tel: +44 1784 497630
Email: ijones@gxt.com

Velocity as an Attribute: Continuous Velocity Estimation from 3D preSDM CRP Gathers.

Ian F.Jones* & Huibert Baud
CGG, 4 Dukes Green Ave, Feltham, Middx, UK, TW14 0LR,
* now at: GX Technology Lawrence House, 45 High Street, Egham, Surrey TW20 9DP

Introduction

Here we present a technique for obtaining high-resolution velocity information from pre-stack time or depth migrated data. Essentially we employ techniques of continuous velocity estimation used for iterative model update (Jones, et al, 1997, 2000), but apply them in a different context. Rather that using the velocity estimator strictly for velocity model building (on a set of sparse lines), we apply the estimation techniques to the common reflection-point (CRP) gathers resulting from the final pre-stack migration for all CRPs in the 3D survey. This achieves two things: firstly it estimates a residual velocity correction for stacking the final CRP gathers to obtain an enhanced image (Jones, et al, 1998a), and secondly, it delivers a dense estimate of velocity for the entire 3D volume in a geologically coherent manner. It is this second feature which is the subject of this paper.

In conventional processing, we usually attempt to 'remove' the effects of velocity from the processing sequence:

- we flatten gathers for stacking or AVO analysis,
- we derive DMO operators which are insensitive to velocity, or
- we construct a macro-model for migration in order to produce flat post-migration gathers.

However, we do not usually use the velocity as a 'deliverable' attribute in its own right. Here we assess if the velocity field can bring useful information, beyond the demands of conventional time or depth processing. It may also be the case that we can derive meaningful information from the velocities (e.g. pressure).

Although the example here was one resulting from a 3D pre-stack depth migration (preSDM) project, we consider that useful information could equally well be obtained from 3D pre-stack time migrated (preSTM) data.

The Method

The basis of the technique is that described by Doicin et al (1995) wherein a common mid-point (CMP) gather is NMO corrected, and then a scan of perturbed residual move-out gathers is created from it. This ensemble of move-out corrected gathers is then input to a coherency analysis routine to determine the 'best' move-out velocity on the basis of say, stack power. This approach results in an estimate of stacking velocity at each CMP location and each time sample. In this regard, their approach was similar to techniques previously described (e.g. de Bazelaire, 1988). However, the important innovation in the work of Doicin et al., was related to the statistical analysis of the information produced so as to eliminate picks of peg-leg multiples, and to eliminate velocity information which showed little or no spatial (geological) coherence.

Further refinement of the dense velocity cube can be achieved by 3D least-squares fitting of the velocities, so as to eliminate statistical outliers (Grubb & Walden, 1995; Adler & Brandwood, 1999).

In this instance, we applied the technique to CRP gathers resulting from 3D preSDM with hyperbolic moveout 're-inserted' into the otherwise flat CRP gathers using inverse NMO, employing the velocity model associated with the migration (Jones et al, 1998a).

It should be noted that no model is input to this process. The procedure is entirely automatic: the output at this stage is in the form of a 3D scatter of RMS values, which show some spatial consistency. It is only when we invert to interval velocities that a model is used.

Results

The example shown is taken from a gas cloud problem associated with a North Sea salt swell (courtesy of Kerr-McGee UK). Here we employ the velocity estimation technique continuously to produce a velocity volume. In figure 1, we see a preSDM seismic section from this 3D survey, after the last iteration of CRP-scan model building and residual move-out (RMO) correction. Here, the velocity-depth model was constructed using the iterative CRP-scan technique (Audebert & Diet, 1996; Jones et al, 1998b) on a 300m by 300m grid, and the RMO correction was estimated continuously on lines separated by 37.5m, sampled every 12.5m along the lines.

Figures 2 & 3 show the interval velocity model for this line resulting from iterative CRP-scan picking, and its corresponding RMS field. In figure 4 we have the RMS velocity profile resulting from the RMO analysis, but prior to edition and smoothing.

At a first glance, it would appear that the velocity structure seen in Fig. 4 is merely a noisy version of the smooth RMS velocity field shown in Fig. 3. However, to correctly assess the high resolution velocity field for meaningful structure, we must look at the velocity changes along an horizon.

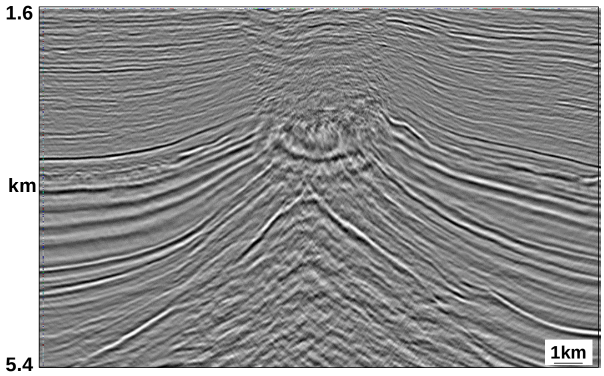

Figure 1: 3D preSDM image from final RMO'd gathers

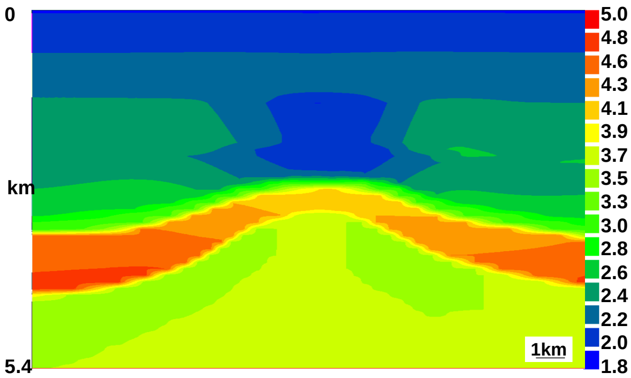

Figure 2: Interval velocity of final model

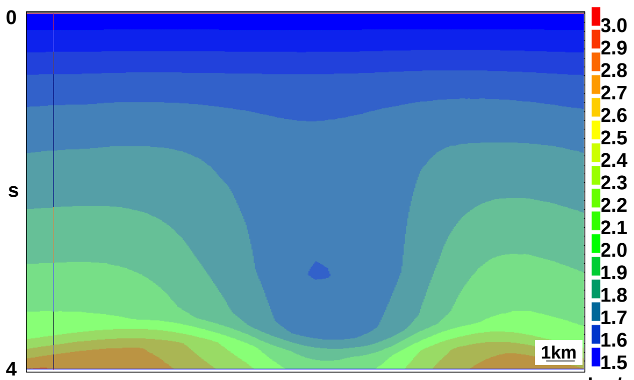

Figure 3: RMS velocity of final model

In order to demonstrate the usefulness of velocity as an attribute, we selected an horizon which showed some detailed amplitude structure. In this case we selected the top Balder event, which clearly exhibited radial faulting. This can be seen on the amplitude map (figure 5).

For the rest of the study, we concentrated our efforts on the section of the horizon denoted in the box, where the faulting is most evident.

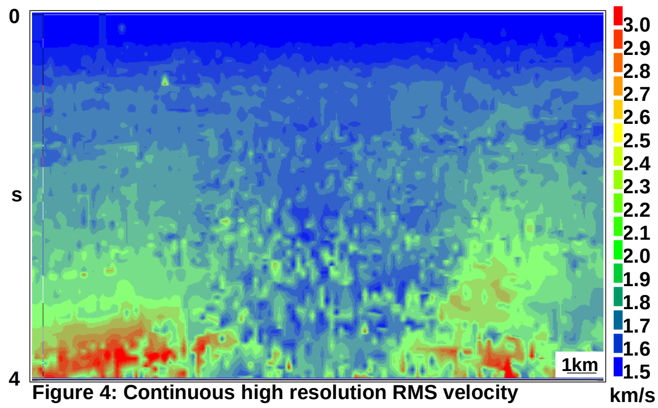

Figure 4: Continuous high resolution RMS velocity (12.5m * 37.5m CRP spacing, 19 point operator)

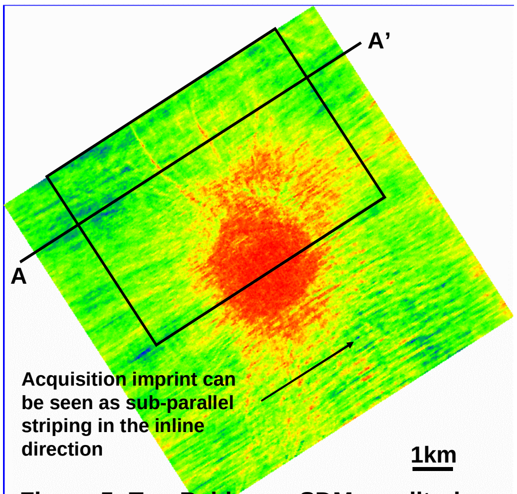

Figure 5: Top Balder preSDM amplitude

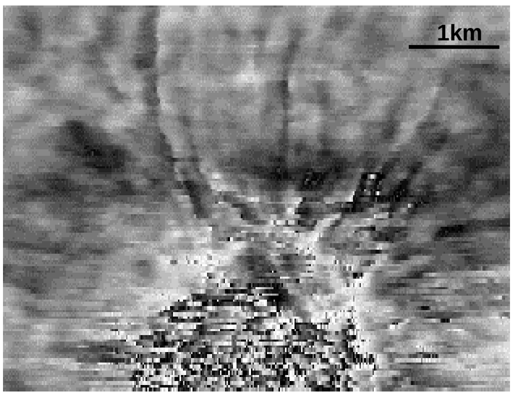

Figure 6: Top Balder Wavelet-transform fault detection

In figure 6 we show the wavelet-transform fault detection result for this horizon (Morlet et al, 1982a&b), and in figure 7, we have superimposed an interpretation of the radial faults emanating from the salt swell, onto the amplitude map. We have also denoted the extent of poor image quality, resulting from the gas cloud, around the centre of the salt swell. In figure 8, we show a vertical seismic section (from line A-A' indicated in figure 7). Faulting at the top Balder can be seen, denoted by the arrow. This corresponds to the main radial fault (left of centre) in figure 7. It should be noted that there is no change in seismic character discernible across the fault.

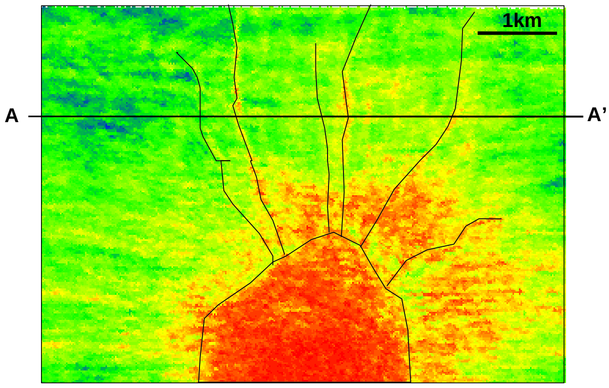

Figure 7: Top Balder preSDM amplitude

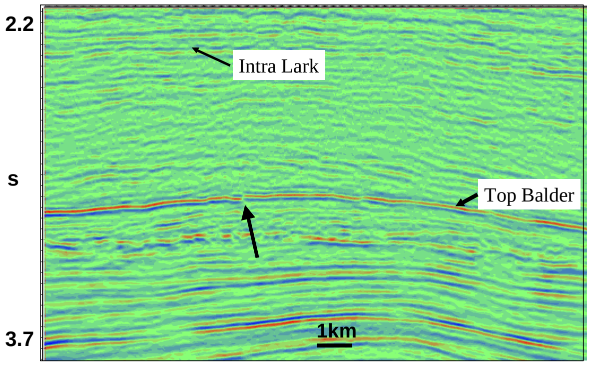

Figure 8: 3D preSDM vertical profile corresponding to line A-A'. Note the faulting visible on the top Balder event (denoted by the arrow)

Figure 9 shows the RMS velocity associated with the final preSDM model for this horizon. Figure 10 shows the corresponding 'high resolution' (HR) RMS velocity estimated on a 12.5m by 37.5m grid. Figures 11 & 12 show the corresponding interval velocity maps, computed between the top Balder and intra Lark horizons (about 700m thick). The fault interpretations from the seismic horizon amplitude maps (of figure 7) are superimposed on the HR velocity result. It should be noted that the faults were interpreted from the seismic amplitudes and *not* from the HR velocity displays.

We can see that the major regions of similar velocity are bounded by the faults. Velocity variations of about 200m/s are apparent over the fault boundaries, and the transition between regions is quite sharp (about 60m transition).

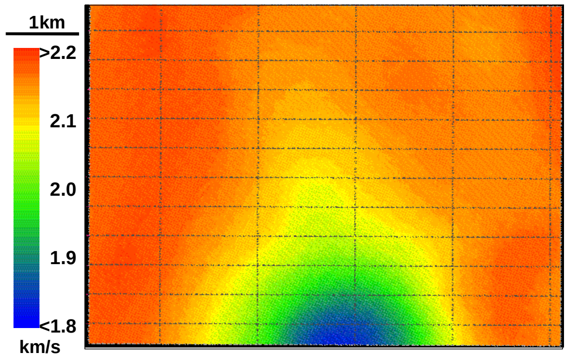

Figure 9:Top Balder RMS velocity smoothed picks: 500*500m grid

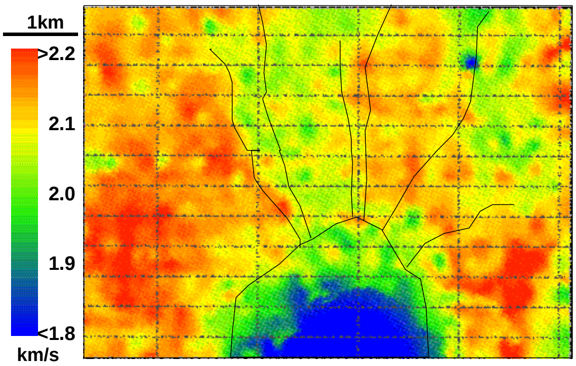

Figure 10: Top Balder high resolution RMS velocity (12.5m * 37.5m CRP spacing, 19 point operator)

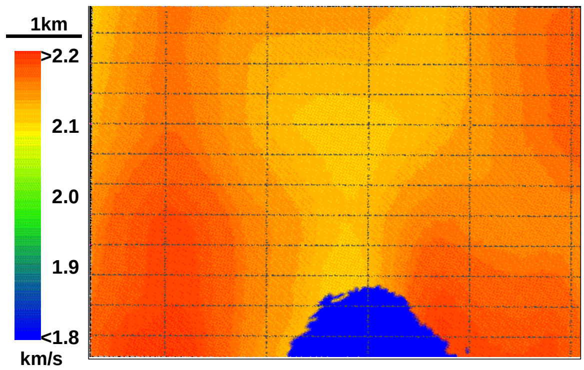

Figure 11: Top Balder interval velocity smoothed picks: 500*500m grid

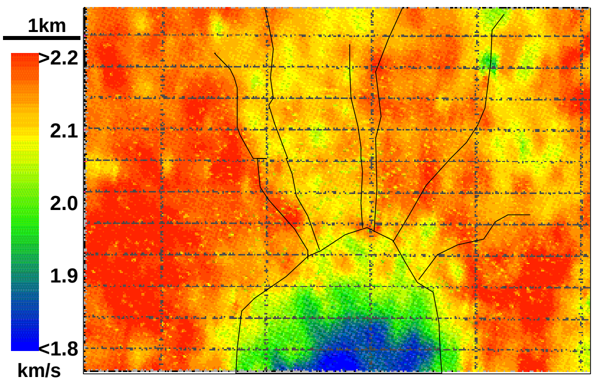

Figure 12: Top Balder high resolution interval velocity (12.5m * 37.5m CRP spacing, 19 point operator)

For comparison, at the depth of the top Balder (3200m), the measured vertical wavelength of the reflection event is about 50m: for migrated data, the lateral Fresnel zone extent should be about equal the dominant wavelength, so this lateral resolution of velocity is not unreasonable.

An estimate of the velocity measurement error was also made for the volumes. On the horizon shown here, the values of standard deviation vary from between ±18m/s – ±45m/s, which represents between about 1 - 2% error on the RMS velocity (figure 13). In this instance, the standard deviation was computed from the velocity estimates within a 'segment'. (A segment being the length over which the amplitudes and velocities display some spatial coherence). This will be a biased indicator, firstly as segment lengths vary, and secondly as the construction of the segments themselves was based on statistical criteria which have rejected outliers and features which did not display lateral coherence. Thus we use the word 'error' loosely in this context.

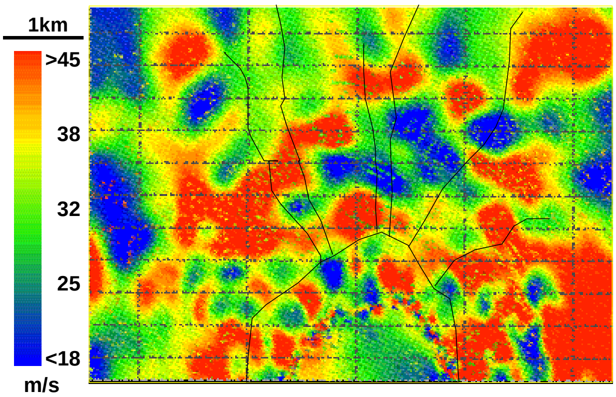

Figure 13: Top Balder high resolution RMS velocity standard deviation

In addition, as this quantity relates to the variation in, and not the accuracy of, the velocity estimated, we must treat these error estimates with caution, and use them more as a comparative diagnostic. In other words, when we estimate the velocity with many values, we only improve the precision of that estimate, but *not* the accuracy. (i.e. if the values coming out from our velocity estimator were all erroneous, but consistently erroneous, then we would simply have a very precise estimate of that inaccurate result).

In this instance, the velocity change across the fault compartment on the left of centre in figure 10, is about 200m/s, whereas the error is maximally ±45m/s. Thus we can conclude that the observed velocity change across the fault is statistically meaningful.

The production project conducted for Kerr McGee also included delivery of a 3D acoustic impedance volume. This was obtained using TDROV, a true 3D acoustic impedance inversion scheme based on simulated annealing (Gluck et al, 1996). TDROV is unique in that it outputs acoustic impedance layers directly. The impedance volume determined from the seismic data can be viewed as an independent estimate of parameter (rho*v), (where rho is the density and v the interval velocity) as compared to the velocity cube. With this in mind, it is legitimate to produce a 3D density estimate from the ratio of acoustic impedance (AI) and interval velocity (Vi).

For comparison to the high-resolution velocity results, we averaged the acoustic impedance micro-layers (figure14) over an interval in the vicinity of top Balder. (The impedance result of figure 14 corresponds to the seismic line shown in figure 8). Taking the ratio of AI/Vi, we then created an average density map for the interval (figure 15).

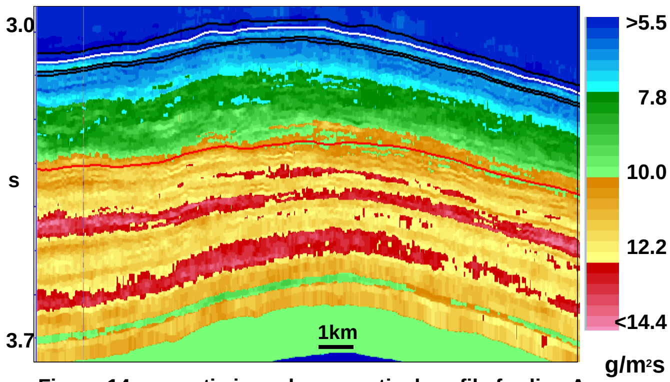

Figure 14: acoustic impedance vertical profile for line A-A' (corresponding to the seismic section in figure 8)

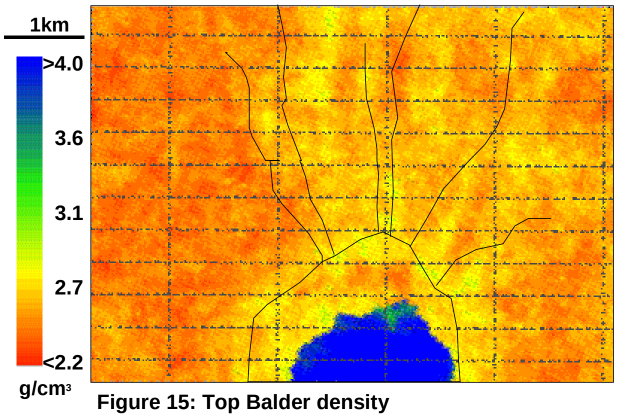

Figure 15: Top Balder density

In this instance, we do not see large variations in density (this layer is predominantly a sand), and the variation in velocity is interpreted as resulting from gas leakage from the reservoir, into the sand layer, being bounded by the faults.

In conjunction with well-log measurements, such high-resolution velocity estimates could be of great value in predicting geo-pressure (Kan, et al, 1999; Lee & Xu, 2000).

Conclusions

It has been previously demonstrated that automated RMO estimation can improve the final image resulting from a preSDM project.

As a corollary to that work, we show here how the same technique can be applied to all pre-stack migrated CRP gathers in a study to deliver a dense velocity cube, and that the interval velocity derived in this way can yield valuable information to the interpreter.

Fault definition (with a resolution comparable to the post-migration Fresnel zone extension) can be achieved from the high-resolution velocity field. This information could be used in conjunction with well information to estimate geo-pressure, and in the case of fault compartmentalised velocity regions seen here, could be a useful guide to the detection of over-pressure, especially for fault bounded compartments.

In addition, these techniques have already been put to use in CGG for combination with geostatistical calibration with well-logs to furnish time-to-depth functions for depthing.

References

Adler, F., & Brandwood, S., 1999: Robust estimation of dense 3D stacking velocities from automated picking, SEG expanded abstracts, SPRO4.6.

Audebert, F., Diet, J.P., 1996, CRP-scans from 3D pre-stack depth migration- a new tool for velocity model building, 58th Ann. Internat. Mtg. Europ. Assoc. Expl. Geophys.

de Bazelaire, E., 1988, Normal move-out revisited: inhomogeneous media and curved interfaces, Geophysics v53, p143.

Doicin, D., Johnson, C., Hargreaves, N., and Perkins, C., 1995, Machine guided velocity interpretation, 57th Ann. Internat. Mtg. Europ. Assoc. Expl. Geophys.

Gluck, S., Juve, E., Lafet, Y., 1996, Multichannel stratigraphic inversion of post-stack seismic data, SEG expanded abstracts, p1793-1796.

Grubb, H.J., & Walden, A.T., 1995, Smoothing seismically derived velocities< Geophysical Prospecting, v43, p1061-1082.

Jones, I.F., Audebert, F., Martin, S., & Ibbotson, K, 1997, Continuous 3D preSDM velocity analysis: 59th Ann. Internat. Mtg. Europ. Assoc. Expl. Geophys.

Jones, I.F., Ibbotson, K., Henry, B., Strachan, A., Baud, H., 1998a, Enhancements to 3D preSDM salt-flank imaging, Journal of Seismic Exploration, v7, No.3/4, pp329-346..

Jones, I.F., Ibbotson, K, Grimshaw, M., & Plasterie, P, 1998b: 3D pre-stack depth migration and velocity model building; The Leading Edge, v17, no.7, p897-911.

Jones, I.F., Baud, H., Ibbotson, K, Audebert, F., 2000, Continuous 3D preSDM velocity analysis: The Leading Edge, March issue, v19, no.3.

Kan T.,K., Kilsdonk, B., West, C., 1999, 3D geopressure analysis in the deepwater Gulf of Mexico. The Leading Edge, v18, No.4.

Lee, W.B., & Xu, W. , 2000, 3D geostatistical velocity modelling: salt imaging in a geopressure environment. The Leading Edge, v19, No.1.

Morlet, J., Arens, G., Fourgeau, E. and Giard, D., 1982a. Wave propagation and sampling theory. Part I: Complex signal and scattering in multilayered media: Geophysics, v47, p203-221.

Morlet, J., Arens, G., Fourgeau, E. and Giard, D., 1982b. Wave propagation and sampling theory. Part II: Sampling theory and complex waves: Geophysics, v47, p222-236.

Acknowledgements

The authors wish to thank Kerr-McGee for kind permission to use their data. Thanks also to Bill Henry, Andy Strachan, and Bruno Gratacos of CGG London.